Carrier recombination in 1.3 μm GaAsSb/GaAs quantum well lasers

K. Hild, S. J. Sweeney,[a] S. Wright, D. A. Lock, S. R. Jin, and I. P. Marko
Advanced Technology Institute, University of Surrey, Guildford, Surrey GU2 7XH, United Kingdom

S. R. Johnson, S. A. Chaparro, S.-Q. Yu, and Y.-H. Zhang
MBE Group, Arizona State University, Tempe, Arizona 85287

(Received 14 August 2006; accepted 19 September 2006; published online 26 October 2006)

In this letter the authors present a comprehensive study of the threshold current and its temperature dependence in GaAsSb-based quantum well edge-emitting lasers for emission at 1.3 μm. It is found that at room temperature, the threshold current is dominated by nonradiative recombination accounting for more than 90% of the total threshold current density. From high hydrostatic pressure dependence measurements, a strong increase in threshold current with pressure is observed, suggesting that the nonradiative recombination process may be attributed to electron overflow into the GaAs/GaAsP barrier layers and, to a lesser extent, to Auger recombination. © *2006 American Institute of Physics*. [DOI: 10.1063/1.2369649]

Lasers emitting close to 1.3 μm are of considerable importance for the development of metro-area networks.[1] Progress in this area has been hindered largely by the need to significantly reduce the cost of the laser module itself. The incumbent InGaAsP quantum well (QW) material system used to make such lasers suffers from two problems: Firstly, the fact that they are grown on InP makes it difficult to produce vertical cavity surface emitting lasers (VCSELs) which are vastly more cost effective but are better suited to GaAs substrates. Secondly, the devices are highly susceptible to temperature variations resulting in the need to incorporate sophisticated temperature control electronics into the package, leading to an order of magnitude increase in cost. Hence, there has been considerable effort devoted to the development of GaAs-based laser active regions which emit at 1.3 μm. InAs quantum dots[2] and GaInNAs-based QWs have been the subject of extensive research. However, the properties of even the best quantum dot lasers are far from ideal, since their threshold current density increases quickly with temperature around room temperature due to nonradiative recombination resulting in a low characteristic temperature, $T_0 \sim 50$ K $[T_0=(d \ln I_{th}/dT)^{-1}]$, similar to that of standard 1.3 μm QW based lasers.[3] P-doped quantum dot lasers can exhibit very high T_0 values (even infinite over a narrow temperature range), but this is achieved at the expense of higher threshold currents compared with undoped devices.[4] For GaInNAs-based QW lasers, it has been shown that even for the best 1.3 μm devices available, approximately 50% of the threshold current at room temperature may be attributed to defect-related recombination.[5] The implications of this on long-term device stability have yet to be fully addressed. Another possibility is the use of GaAsSb/GaAs QWs.[6] Lasers based upon this material have been produced,[7] but little, if any, research has been undertaken to assess the carrier recombination and temperature dependent processes occurring in such devices. The aim of this letter is to consider the characteristics of GaAsSb/GaAs-based edge-emitting lasers and to explore the potential of GaAsSb/GaAs active regions for use in 1.3 μm VCSELs.

The devices in this study consist of a triple $GaAs_{0.9}P_{0.1}/GaAs/GaAs_{0.7}Sb_{0.3}/GaAs/GaAs_{0.9}P_{0.1}$ (9 nm/5 nm/7 nm/5 nm/9 nm) strain compensated QW active region grown at 585 °C by molecular beam epitaxy. The nominal 30% Sb concentration is estimated based on photoluminescence measurements. The GaAsP layers provide strain compensation to increase the maximum number of highly strained QWs that can be grown pseudomorphically and to reduce strain driven in-plane Sb segregation that leads to inhomogeneous linewidth broadening. The active region is sandwiched between two 20 nm $Al_{0.25}Ga_{0.75}As$ layers, two 150 nm graded-index (GRIN) AlGaAs layer with Al concentration linearly increased from 25% to 65%, one 2 μm *n*-type (Si doped, 2×10^{18} cm^{-3}) $Al_{0.65}Ga_{0.35}As$ cladding layer followed by 500 nm GaAs buffer layer at bottom, and one 2 μm *p*-type (Be doped, 2×10^{18} cm^{-3}) $Al_{0.65}Ga_{0.35}As$ cladding layer followed by 100 nm GaAs cap layer at top. The doping concentration is decreased from 2×10^{18} to 1×10^{17} in both GRIN layers from cladding layer to active region and is increased to 2×10^{19} in GaAs cap layer from cladding layer to surface. The devices are fabricated using a typical broad contact edge-emitting laser process. The device ridges (50 and 100 μm wide) were defined using photolithography and inductively coupled plasma dry etching. By etching down through the *p*-GaAs contact layer and stopping about 0.1 μm above the active region, these ridges provide current confinement as well as waveguiding. Ti/Pt/Au *p*-contact stripes ranging from 40 to 90 μm were deposited using a second mask, after which the wafers are lapped down to 100 μm and AuGe/Ni/Au *n*-metal contacts are deposited on the backside of the substrate; this is followed by rapid thermal annealing for both metal contacts. The devices were measured as cleaved. Their room temperature emission wavelength was measured to be 1.27 μm.

Temperature dependence measurements were performed with a standard closed cycle cryostat setup over the temperature range of 60–290 K. The lasers were driven under pulsed operation with 200 ns long pulses at a duty cycle of 10 kHz in order to minimize Joule heating effects. We investigated the temperature and current dependencies of the spontaneous emission spectra from which we extracted the radiative current (since the integrated spontaneous emission is propor-

[a]Author to whom correspondence should be addressed; electronic mail: s.sweeney@surrey.ac.uk

0003-6951/2006/89(17)/173509/3/$23.00

© 2006 American Institute of Physics
Downloaded 30 Mar 2009 to 131.227.178.132. Redistribution subject to AIP license or copyright; see http://apl.aip.org/apl/copyright.jsp

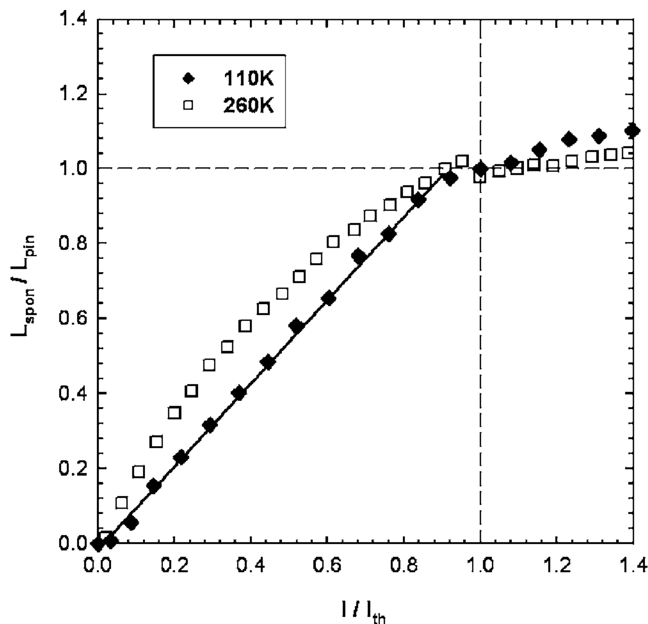

FIG. 1. Integrated spontaneous emission as a function of current at 110 K (solid diamonds) and 260 K (open squares). At 110 K L_{spon} increases linearly with current, indicating that it is dominated by radiative recombination. The contrasting sublinear behavior at higher temperatures indicates the presence of a nonradiative process. Note that at each temperature, L_{spon} has been normalized to its value at threshold (L_{pin}). The lines are guides to the eye.

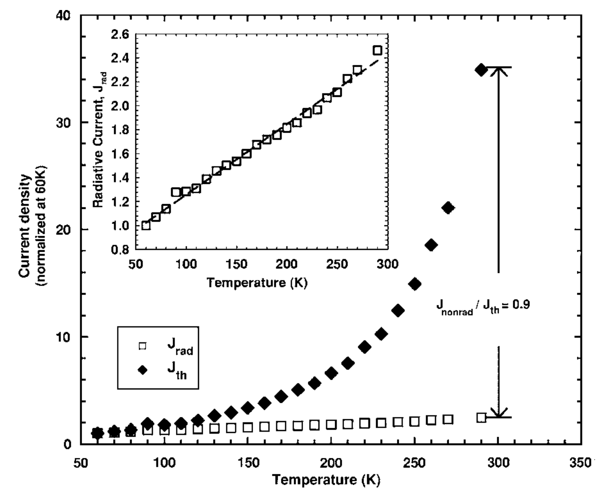

FIG. 2. J_{th} and J_{rad} as a function of temperature (normalized at 60 K). The inset shows the temperature dependence of J_{rad} on an expanded scale from which it can be seen to exhibit an ideal QW-like linear temperature dependence (indicated by the dashed line).

tional to the radiative current). To measure the spontaneous emission, we milled a window in the *n* side of the devices and aligned an optical fiber to collect the spontaneous emission. This technique is described in detail elsewhere.[8] Hydrostatic pressure measurements were also performed on the devices. The application of high hydrostatic pressure causes an increase in the direct band gap, mimicking the effect of alloying, thereby allowing one to investigate wavelength dependent properties of semiconductor lasers. It can also be used to vary the alignment between direct (Γ) and indirect (X, L) bands and to alter the band offsets between layers which have different pressure coefficients.[9] In this work, hydrostatic pressure measurements were performed over the range of 0–8 kbar using a gas compressor system.

The integrated spontaneous emission (L_{spon}) versus current at two different temperatures, 110 and 260 K, is shown in Fig. 1. In both cases the integrated spontaneous emission pins at threshold due to the fact that the carrier density is clamped by the lasing process. The two curves have been normalized to the value of L_{spon} at threshold ($=L_{pin}$), so that the subthreshold shape of both curves can be easily compared and contrasted. There is a clear difference in the behavior of the device at the two temperatures. At 110 K, the subthreshold L_{spon} versus current curve is linear, suggesting that the primary current path flowing through the laser may be associated with radiative recombination. Furthermore, the fact that the curve remains linear down to low currents suggests that defect-related recombination makes a relatively small contribution to the threshold current. In stark contrast, the sublinear behavior of the L_{spon} versus current curve at 260 K suggests that a nonradiative process is present and that this process has a stronger carrier density dependence than the radiative current.

In Fig. 2 we show the normalized (at 60 K) temperature dependence of the threshold current density J_{th} (diamonds). We find that the devices are highly temperature sensitive with a characteristic temperature $T_0 \sim 60-70$ K at RT comparable to values that have been reported elsewhere for GaAsSb/GaAs devices[7] and InGaAs(P)/InP devices[8] emitting around 1.3 μm. From measurements on probed broad area devices at 300 K, we estimate J_{th} to be ~1.6 kA cm^{-2} Also shown in Fig. 2 is the temperature dependence of the radiative current density J_{rad} (squares), which was found from the pinning level of the integrated spontaneous emission, L_{pin}, as seen in Fig. 1, since at threshold $L_{pin} \propto J_{rad}$. From this, we estimate that at 290 K the radiative recombination process accounts for ~10% of the total threshold current. Clearly, nonradiative processes dominate and account for ~90% of J_{th} close to RT. From the inset in Fig. 2, it can also be seen that J_{rad} has the ideal QW linear temperature dependence,[10] leading to the conclusion that the loss mechanism(s) must increase superlinearly with increasing temperature.

Further evidence for the importance of nonradiative recombination may be found from high pressure measurements. Figure 3 shows the measured room temperature pressure dependence of J_{th} for the GaAsSb devices (circles). Also shown is the ideal expected variation of $J_{rad} \propto E_g^2$ (Ref. 11) (dot-dot-dashed line), where E_g is the band gap (taken from $E_g = hc/\lambda_{lasing}$, where λ_{lasing} is the measured lasing wavelength). Note that in each case, J_{th} and J_{rad} have been normalized to their respective values at atmospheric pressure. Clearly, it can be seen that J_{th} increases more rapidly with pressure than the ideal J_{rad}. Preliminary pressure measurements suggest that the pressure dependence of J_{rad} in our devices is very close to ideal.[12] From the earlier temperature dependence measurements, we found that a nonradiative process dominated at room temperature forming ~90% J_{th}. We therefore conclude that the observed strong increase of J_{th} with pressure is due to nonradiative recombination. The conduction band offset of the GaAsSb/GaAs interface (for 30% Sb) is still a matter of debate with reports in the literature of both weak type I (Ref. 13) and type II alignments.[14] This indicates that the conduction band offset is close to zero. Due to the slightly larger pressure coefficient of the GaAsSb (Ref. 15) QW Γ minimum compared to the GaAs barrier Γ minimum[16] (difference=+1.2 meV/kbar), occupation of

Downloaded 30 Mar 2009 to 131.227.178.132. Redistribution subject to AIP license or copyright; see http://apl.aip.org/apl/copyright.jsp

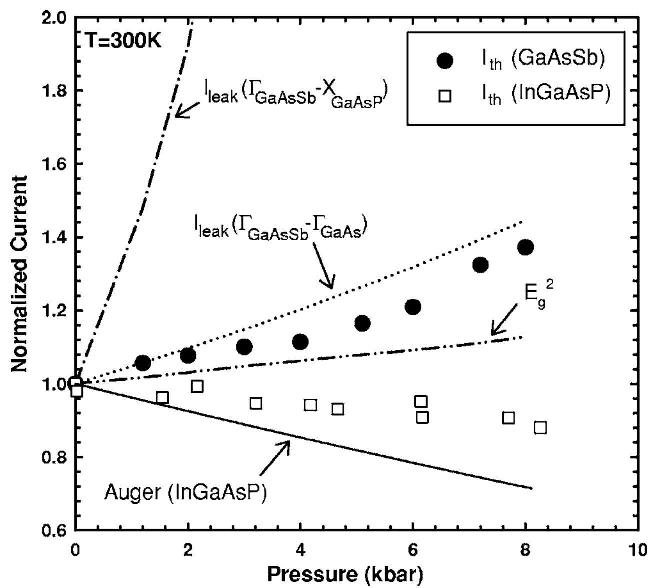

FIG. 3. Measured pressure dependence of J_{th} for the GaAsSb devices (closed circles) and ideal J_{rad} (E_g^2 dependence) (dot-dot-dashed line), normalized at atmospheric pressure. The dotted line indicates the calculated pressure dependence of carrier leakage into the GaAs Γ minimum, while the dot-dashed line indicates the pressure variation of carrier leakage into the X minima of the GaAsP layers. For comparison, the pressure dependence of J_{th} for a 1.3 μm InGaAsP device is shown (open squares) together with the calculated variation in the Auger current with pressure for the InGaAsP device (solid line) (derived from Ref. 17).

electrons in the GaAs barrier states will increase with increasing pressure, as shown by the calculated dotted line in Fig. 3. Furthermore, due to the small or possibly negative (type II) GaAsSb/GaAs band offset, the GaAsP layers act as additional barriers. With increasing pressure, the X minima in the GaAsP layers move to lower energy and may provide an additional leakage path, as shown by the dot-dashed line in Fig. 3. Thus, for a fixed quasi-Fermi-level splitting, the occupation of the barrier layers will increase exponentially with increasing pressure leading to an increased leakage current. While carrier leakage into the GaAs and/or GaAsP barrier layers offers a possible explanation for the increase of J_{th} with pressure, it is clear that this in itself is insufficient. The lower rate of increase of J_{th} with pressure dependence compared to the leakage paths may be explained if carrier leakage and a nonradiative process that decreases with pressure are *both* present. In Fig. 3 for comparison we plot the pressure dependence of J_{th} (open squares) and the Auger current (solid line) for a typical 1.3 μm InGaAsP device (taken from Ref. 17). For the InGaAsP devices, Auger recombination is the dominant nonradiative process[8,10,17,18] causing J_{th} to reduce with pressure due to the decrease in the Auger current with pressure. We therefore propose that the nonradiative recombination current which dominates J_{th} for the GaAsSb devices at room temperature is due to a combination of carrier leakage and Auger recombination. However, based on our data, it is not yet possible to quantify the role of each of these nonradiative current paths.

In summary, from our first studies of 1.3 μm GaAsSb lasers, we find that at room temperature the threshold current is dominated by nonradiative recombination. The nonradiative process is also responsible for the poor temperature sensitivity of the devices resulting in low T_0 values around room temperature. From our pressure dependence measurements, we observe that the threshold current increases with pressure, consistent with the transfer of carriers into the GaAs/GaAsP barrier layers due to the decrease of the band offset with pressure. This suggests that carrier overflow into the GaAs and/or GaAsP barrier layers together with Auger recombination forms a large nonradiative current path in these devices at normal operating temperatures.

The authors thank E. P. O'Reilly and S. B. Healy (Tyndall Institute, Ireland) for useful discussions. They also gratefully acknowledge EPSRC (UK) for supporting this project under Grant No. GR/T21516/01.

[1]T. P. McGarty and G. J. Clancy, Jr., IEEE J. Sel. Areas Commun. **1**, 816 (1983).
[2]O. B. Shchekin and D. G. Deppe, IEEE Photonics Technol. Lett. **14**, 1231 (2002).
[3]I. P. Marko, A. R. Adams, S. J. Sweeney, I. R. Sellers, D. J. Mowbray, M. S. Skolnick, H. Y. Liu, and K. M. Groom, IEEE J. Sel. Top. Quantum Electron. **11**, 1041 (2005).
[4]I. P. Marko, N. F. Masse, S. J. Sweeney, A. D. Andreev, A. R. Adams, N. Hatori, and M. Sugawara, Appl. Phys. Lett. **87**, 211114 (2005).
[5]S. Tomic, E. P. O'Reilly, R. Fehse, S. J. Sweeney, A. R. Adams, A. D. Andreev, S. A. Choulis, T. J. C. Hosea, and H. Riechert, IEEE J. Sel. Top. Quantum Electron. **9**, 1228 (2003).
[6]T. Anan, K. Nishi, S. Sugou, M. Yamada, K. Toukutome, and A. Gomyo, Electron. Lett. **34**, 2127 (1998).
[7]M. Yamada, T. Anan, K. Toukutome, A. Kamei, K. Nishi, and S. Sugou, IEEE Photonics Technol. Lett. **12**, 774 (2000).
[8]S. J. Sweeney, A. F. Philips, A. R. Adams, E. P. O'Reilly, and P. J. A. Thijs, IEEE Photonics Technol. Lett. **10**, 1076 (1998).
[9]D. J. Wolford, T. F. Kuech, J. A. Bradley, M. A. Gell, D. Ninno, and M. Jaros, J. Vac. Sci. Technol. B **4**, 1043 (1986).
[10]E. P. O'Reilly and M. Silver, Appl. Phys. Lett. **63**, 3318 (1993).
[11]A. R. Adams, M. Silver, and J. Allam, Semicond. Semimetals **55**, 301 (1998).
[12]K. Hild, S. J. Sweeney, I. P. Marko, S. R. Jin, S. R. Johnson, S. A. Chaparro, S. Yu, and Y.-H. Zhang, Phys. Status Solidi B (to be published).
[13]J.-B. Wang, S. R. Johnson, S. A. Chaparro, D. Ding, Y. Cao, Yu. G. Dadofyev, Y.-H. Zhang, J. A. Gupta, and C. Z. Guo, Phys. Rev. B **70**, 195339 (2004).
[14]Q. Liu, S. Derksen, A. Lindner, F. Scheffer, W. Prost, and F.-J. Tegude, J. Appl. Phys. **77**, 1154 (1994).
[15]A. D. Prins, D. J. Dunstan, J. D. Lambkin, E. P. O'Reilly, A. R. Adams, R. Pritchard, W. S. Truscott, and K. E. Singer, Phys. Rev. B **47**, 2191 (1993).
[16]D. J. Wolford and J. A. Bradley, Solid State Commun. **53**, 1069 (1985).
[17]A. F. Phillips, S. J. Sweeney, A. R. Adams, and P. J. A. Thijs, Phys. Status Solidi B **211**, 513 (1999).
[18]M. Silver, E. P. O'Reilly, and A. R. Adams, IEEE J. Quantum Electron. **9**, 1557 (1998).

Downloaded 30 Mar 2009 to 131.227.178.132. Redistribution subject to AIP license or copyright; see http://apl.aip.org/apl/copyright.jsp